Journal of Electroanalytical Chemistry 736 (2015) 8–15

Contents lists available at ScienceDirect

Journal of Electroanalytical Chemistry

journal homepage: www.elsevier.com/locate/jelechem

New electrode architectures based on poly(methylene green) and functionalized carbon nanotubes: Characterization and application to detection of acetaminophen and pyridoxine

Madalina M. Barsan [a], Camilla T. Toledo [a,b], Christopher M.A. Brett [a,*]

[a] Departamento de Química, Faculdade de Ciências e Tecnologia, Universidade de Coimbra, 3004-535 Coimbra, Portugal
[b] Instituto de Ciência e Tecnologia, Universidade Federal dos Vales do Jequitinhonha e Mucuri, Diamantina, MG, Brazil

ARTICLE INFO

Article history:
Received 15 September 2014
Received in revised form 16 October 2014
Accepted 23 October 2014
Available online 30 October 2014

Keywords:
Poly(methylene green)
Composite electrodes
Carbon nanotubes
Acetaminophen
Pyridoxine

ABSTRACT

New electrode platforms have been constructed containing the redox polymer poly(methylene green) (PMG) and functionalized carbon nanotubes (*f*CNT) in two configurations, the first containing MG electropolymerised on a graphite composite electrode (CE) and covered with *f*CNT (*f*CNT/PMG/CE), the second having the MG electropolymerised on top of *f*CNT modified CE (PMG/*f*CNT/CE). Modified electrodes with both configurations were characterized by cyclic voltammetry and electrochemical impedance spectroscopy, and compared with PMG/CE and *f*CNT/CE and CE, in order to evaluate the role of each component in the modified electrode architecture. The modified electrodes were applied to the detection of acetaminophen and pyridoxine, by fixed potential amperometry and differential pulse voltammetry, the latter allowing the simultaneous detection of both analytes. The analytical properties of *f*CNT/PMG/CE and PMG/*f*CNT/CE sensors were obtained and the best analytical performance compared with recently reported acetaminophen and pyridoxine sensors. Determination of both analytes in pharmaceutical samples was successfully performed.

1. Introduction

Electroactive polymers comprise a relatively new class of organic materials, which exhibit both electronic and ionic conductivity. The best way to prepare films of electroactive polymer is by electropolymerisation of the redox-active monomer, as is the case of phenazine monomers [1]. Electropolymerised films of phenazines have been extensively used in electrochemical sensors and biosensors [2], poly(methylene green) (PMG) being mostly utilized for electrocatalysis of NAD^+ regeneration [3–5], and consequently for the development of biofuel cells based on NAD^+-dependent dehydrogenase enzymes [6–11]. PMG's catalytic activity can be attributed to its structure, being similar to flavonoids, natural antioxidants responsible for many catalytic oxidation in nature [12], and because its half wave potential is more positive than that of NADH [11].

Carbon nanotubes (CNT) are now widely known as excellent materials for the construction of electrochemical sensors leading to improved analytical properties, compared with many other carbon materials, such as higher sensitivity, lower limit of detection, due to their enhanced electronic properties, a large edge plane/basal plane ratio, and faster electrode kinetics [13]. CNT have been also used together with PMG, synergetic effects having been demonstrated in dehydrogenase-based reagentless biosensors [14], in a malate dehydrogenase "bucky" paper anode [6], in ethanol/air biofuel cells [9], and in a glucose dehydrogenase based bioanode [9].

The present work focuses on the development and characterization of new electrode architectures based on the redox polymer poly(methylene green) and functionalized CNT (*f*CNT) on graphite-epoxy composite electrode (CE) substrates, containing PMG covered with *f*CNT (*f*CNT/PMG/CE), or with PMG on top of *f*CNT (PMG/*f*CNT/CE). Epoxy composite electrodes have been previously used successfully as electrode substrates in many applications e.g. [15–17]. CNT were first functionalized in nitric acid, to increase their hydrophilicity and introduce functional groups [18], and then dispersed in a chitosan matrix, a biopolymer with good adhesion on solid substrates, high water and anion/cation permeability, high mechanical strength and excellent film-forming ability [19]. The modified electrodes were characterized by cyclic voltammetry and electrochemical impedance spectroscopy (EIS), and then applied to the determination of acetaminophen and pyridoxine,

* Corresponding author. Tel.: +351 239854470; fax: +351 239827703.
E-mail address: cbrett@ci.uc.pt (C.M.A. Brett).

http://dx.doi.org/10.1016/j.jelechem.2014.10.026
1572-6657/

exploring the benefits of modification by both *f*CNT and PMG. Acetaminophen (paracetamol, N-acetyl-p-aminophenol), is a widely used analgesic anti-pyretic drug, [20], its electrochemical detection using CNT being successfully demonstrated e.g. [21], and it was determined here by differential pulse voltammetry (DPV) and fixed potential amperometry. Pyridoxine, one of the compounds of the vitamin B6 group, was also electrochemically determined; several methods exist for the determination of vitamin B6 in pharmaceutical formulations [22], electrochemical ones also having been reported [23–26].

2. Experimental

2.1. Reagents and solutions

All reagents were of analytical grade and were used without further purification. Millipore Milli-Q nanopure water (resistivity $\geqslant$ 18 MΩ cm) was used for the preparation of all solutions.

Methylene green, potassium hexacyanoferrate(II), potassium nitrate were from Fluka, chitosan (low molecular weight), sodium and potassium chloride, acetaminophen (ACOP), pyridoxine, monobasic and dibasic sodium phosphate were from Sigma and sodium tetraborate from May & Baker.

Polymerization of MG was carried out in a solution containing 1.0 mM MG dissolved in 0.025 M $Na_2B_4O_7$ + 0.1 M KNO_3, pH 9.2.

The determination of acetaminophen and pyridoxine was done in sodium phosphate buffer saline 0.1 M NaPBS, containing 0.1 M Na_2HPO_4/NaH_2PO_4 + 0.05 M NaCl, pH 7.0.

2.2. Instrumentation

Electrochemical experiments were performed in a three electrode cell, containing the composite electrode (CE) (area 0.126 cm^2) as working electrode, a Pt wire counter electrode and an SCE reference electrode, using a potentiostat/galvanostat μ-Autolab system (Metrohm-Autolab, Netherlands).

EIS experiments were carried out by using a PC-controlled Solartron 1250 Frequency Response Analyzer, coupled to a Solartron 1286 Electrochemical Interface using ZPlot 2.4 software (Solartron Analytical, UK), with an rms perturbation of 10 mV applied over the frequency range 65.5 kHz–0.1 Hz, with 10 frequency values per frequency decade.

The pH measurements were carried out with a CRISON 2001 micro pH-meter (Crison Instruments SA, Barcelona, Spain).

All experiments were carried out a room temperature (25 ± 1 °C).

2.3. Preparation of modified graphite-epoxy composite electrodes

Graphite-epoxy electrodes were prepared using graphite powder and Araldit epoxy resin/hardener as described previously [27]. Before each use, the surface of the composite electrode was wetted with Milli-Q water and then thoroughly smoothed, first with abrasive paper and then with polishing paper, (Kemet, UK).

Multi-walled CNT (MWCNT) were purified and functionalized as described elsewhere [28]. First, a dispersion of CNT in 3 M nitric acid solution was stirred for 20 h, the solid product was collected on a filter paper and washed until the filtrate solution became neutral. The *f*CNT obtained were then dried in an oven at 80 °C for 24 h. A dispersion of 1% *f*CNT was prepared in 1.0% m/m chitosan (Chit) dissolved in 1.0% v/v acetic acid. A volume of 10 μl of this dispersion was dropped two times on the surface of CE or PMG/CE, leaving to dry each time for ~60 min.

MG was electropolymerised on CE or on *f*CNT/CE from 1.0 mM MG dissolved in 0.025 M $Na_2B_4O_7$ + 0.1 M KNO_3, pH 9.2 by cycling the potential at 50 mV s^{-1}, for 40 cycles, between −0.5 and +1.0 V vs. SCE, for the CE, and between −0.6 and +1.0 V vs. SCE for *f*CNT/CE [29]. The electrodes were left to dry for at least 24 h before use.

2.4. Sample preparation

Acetaminophen and pyridoxine tablets were first finely ground in a mortar and then an appropriate amount was weighed and dissolved in 0.1 M NaPBS buffer to form 66.0 mM and 29.6 mM acetaminophen and pyridoxine solutions, respectively.

3. Results and discussion

3.1. Electropolymerization of MG on CE and *f*CNT/CE and CV characterization of *f*CNT/PMG/CE and PMG/*f*CNT/CE

PMG polymer was deposited on CE and *f*CNT/CE by potential cycling, in a solution containing MG monomer; CVs recorded during polymerization are displayed in Fig. 1. Polymerization begins with the formation of cation radicals at potentials close to +1.0 V vs. SCE, similar to other phenazine monomers [2]. On both substrates, CE and *f*CNT/CE, there is increase in oxidation/reduction polymer peak currents with each polymerization cycle, the potentials of which coincide with the monomer peaks. On *f*CNT/CE (Fig. 1b) the currents are significantly higher, due to the higher surface area of *f*CNTs and the polymer is better formed, the

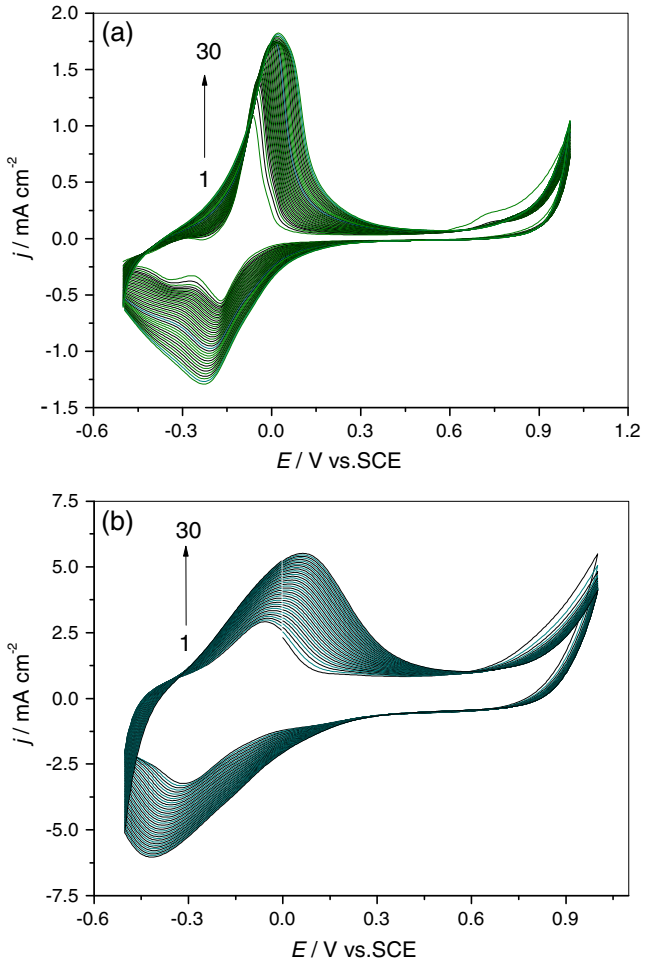

Fig. 1. CV-s recorded during the polymerization of MG on (a) CE and (b) *f*CNT/CE from a solution containing 1 mM MG in 0.025 M $Na_2B_4O_7$ + 0.1 M KNO_3, pH 9.25; v = 50 mV s^{-1}.

oxidation/reduction peak currents increasing up to 5.5 and −6.1 mA cm^{-2}, respectively, while on CE (Fig. 1a) they increased to 1.9, and −1.3 mA cm^{-2}. However, the larger peak separation on *f*CNT suggests that the PMG redox process is less reversible than on CE. Both *f*CNT/PMG/CE and PMG/*f*CNT/CE modified electrodes were very robust, the current decrease upon continuous potential cycling being negligible less than 4% of the initial value after 100 cycles. This is probably due to interactions between CNT and PMG, which may be either electrostatic, since CNT possess carboxylate groups and PMG has a quaternary amino group and a sulfur anion, or π-π and hydrophobic interactions, similar to those between thionine, which has a very similar structure to PMG, and CNT [30].

The variation of peak currents with scan rate (see Fig. 2) revealed that the overall electrochemical processes are diffusion controlled on both PMG/*f*CNT/CE and *f*CNT/PMG/CE, that can be attributed to the rate-determining step being diffusion of counterions into the polymer structures. For the electrode PMG/*f*CNT/CE (Fig. 2b$_2$), the slope of the plots of I_p vs. $v^{1/2}$ are 15.9 and 17.3 mA cm^{-2} (V s^{-1})$^{-1/2}$, for the anodic and cathodic processes respectively, more than 3 times higher than for *f*CNT/PMG/CE (Fig. 2a$_{1,2}$) indicating a larger accessible surface area at PMG/*f*CNT/CE. If *f*CNT is deposited first on the CE, then the formation of PMG from MG monomer can occur also on the CNT within the CNT network, thus providing a higher surface area for polymer deposition than in the case of *f*CNT/PMG/CE.

3.2. Electrochemical impedance spectroscopy

Electrochemical impedance spectroscopy was used to examine the interfacial properties of the unmodified composite electrodes, of CE modified with *f*CNTs or PMG alone and *f*CNT together with PMG in both configuration PMG/*f*CNT/CE and *f*CNT/PMG/CE. The measurements were performed in 0.1 M KCl solution at 0.0 V vs. SCE, chosen in the electroactive potential range of PMG.

As observed from Fig. 3, the modification of CE with either *f*CNT, PMG or *f*CNT and PMG together, all lead to a very large decrease in the impedance value, from 5 kΩ cm^2 for bare CE, to 200 for PMG/CE and less than 100 Ω cm^2 for the other modified composite electrodes. The spectra recorded at electrodes with *f*CNT, i.e. at *f*CNT/CE, *f*CNT/PMG/CE and PMG/*f*CNT/CE in Fig. 3a–c are very similar in the low frequency region, being represented by capacitive lines, in the high frequency region the difference being that when PMG is present, the spectra begin with a small diameter semicircle, correlated with charge transfer reactions of the redox polymer. The spectrum of PMG/CE without CNT was different, having a slightly higher impedance, and diffusion control over a wider frequency range.

The spectra were fitted by using the equivalent circuit presented in Fig. 3d. This circuit comprises a cell resistance, R_Ω, in series with a parallel combination of a charge transfer resistance, R_{ct}, and a double layer non-ideal capacitance, expressed as a constant phase element, CPE$_{dl}$ (to fit the semicircle in the high frequency region of the spectra). This parallel combination is in series with a Warburg resistance, Z_w (for intermediate frequency) and a film capacitance, CPE$_f$ (for the low frequency region). CPE = $[(Ci\omega)^\alpha]^{-1}$, is a non-ideal capacitor, due to the porosity and non-homogeneity of the surface, with $0.5 < \alpha < 1$. The Open Warburg Element, $Z_{W,}$ is expressed by: $Z_W = R_W\ \mathrm{cth}[(\tau i\omega)^\alpha](\tau i\omega)^{-\alpha}$, where $\alpha < 0.5$, τ is the diffusional time constant and R_W the diffusional resistance [31].

Data obtained by fitting the spectra are shown in Table 1. As can be seen, the presence of *f*CNT leads to an increase in double layer CPE, CPE$_{dl}$, of the PMG/CE, both *f*CNT/PMG/CE and PMG/*f*CNT/CE

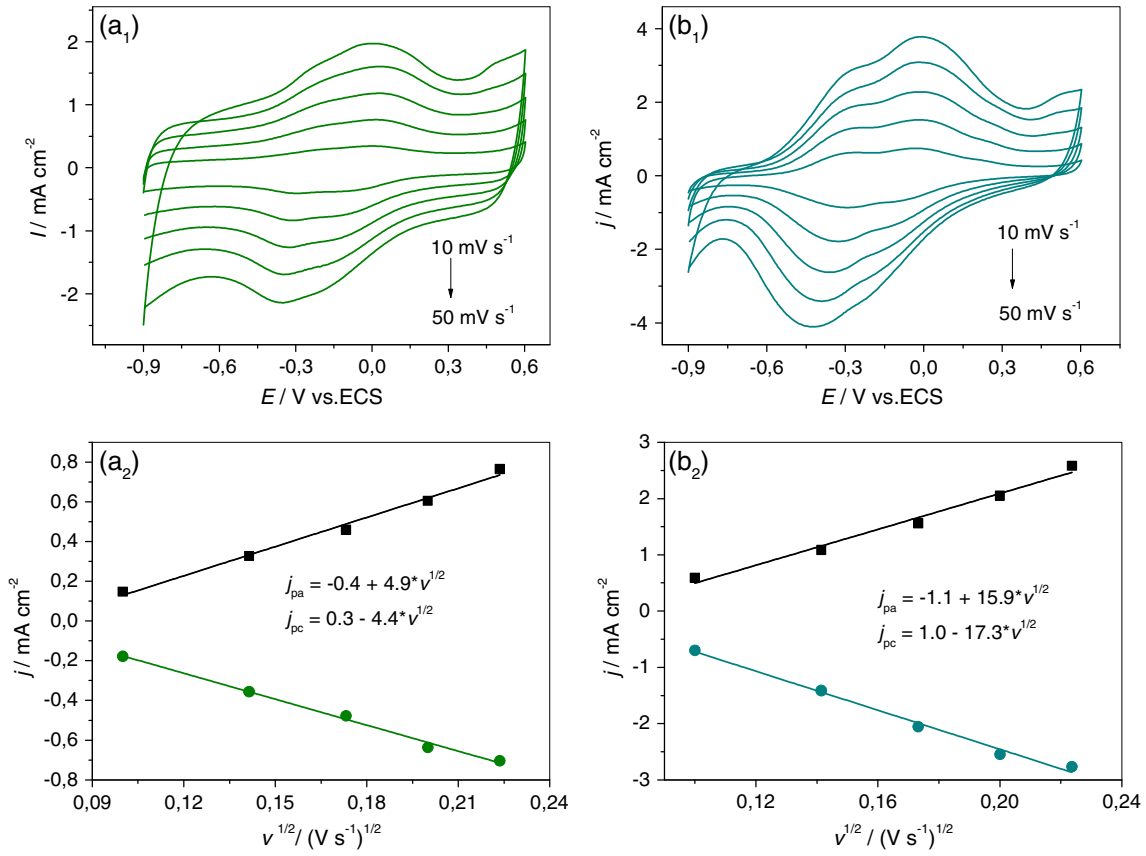

Fig. 2. CV-s recorded in 0.1 M KCl at (a$_1$) *f*CNT/PMG/CE and (b$_1$) PMG/*f*CNT/CE at different scan rates from 10 to 50 mV s^{-1}; (a$_2$) and (b$_2$), corresponding linear plots of peak current vs. $v^{1/2}$.

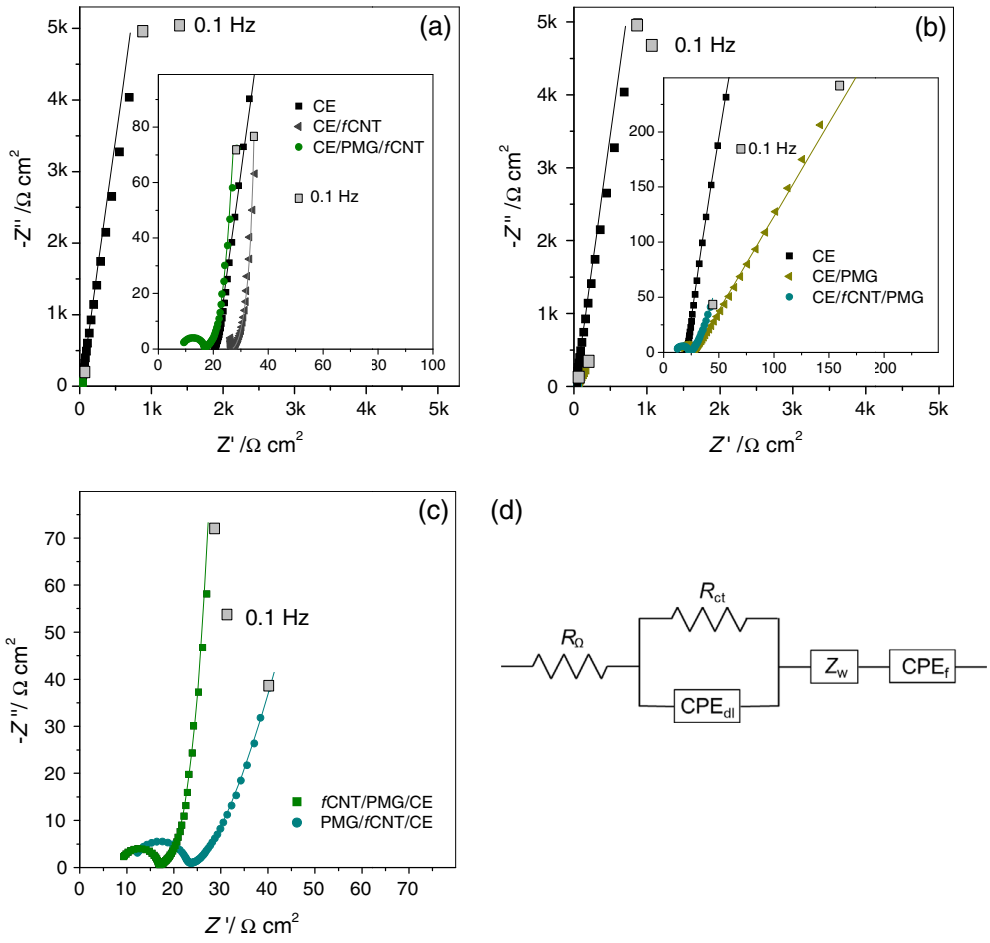

Fig. 3. Complex plane impedance spectra recorded in 0.1 M KCl at 0.0 V vs. SCE at (a) CE, *f*CNT/CE and *f*CNT/PMG/CE, (b) CE, PMG/CE and PMG/*f*CNT/CE, (c) *f*CNT/PMG/CE and PMG/*f*CNT/CE, and (d) equivalent circuit used to fit the spectra.

Table 1
Equivalent circuit components values extracted by fitting the spectra in Fig. 3a–c to the equivalent circuit in Fig. 3d.

Electrode	R_{ct}/Ω cm^2	CPE_{dl}/μF cm^{-2} s$^{\alpha-1}$	α_1	Z_W/Ω cm^2 s$^{\alpha-1}$	τ/ms	α_2	CPE_f/mF cm^{-2} s$^{\alpha-1}$	α_3
CE	–	275.7	0.91	–	–	–	–	–
*f*CNT/CE	–	–	–	2.4	24	0.35	19.1	1.00
PMG/CE	9.3	1.2	1.00	–	–	–	2.2	0.79
*f*CNT/PMG/CE	8.1	2.0	0.95	0.7	20	0.29	23.8	1.00
PMG/*f*CNT/CE	11.3	1.8	0.94	1.3	22	0.29	47.3	0.94

having higher CPE_{dl} values, of 2.0 and 1.8, respectively, than 1.2 μF cm^{-2} s$^{\alpha-1}$ at PMG/CE. This is probably mostly the effect of increased surface area, since normalization of the impedance spectra is done by electrode geometric area. The CPE values attributed to the film, CPE_f, are increased by PMG together with CNT in both configurations, increasing from 2.2 mF cm^{-2} s$^{\alpha-1}$ for PMG/CE to 23.8 and 47.3 mF cm^{-2} s$^{\alpha-1}$ for *f*CNT/PMG/CE and PMG/*f*CNT/CE, respectively. Moreover, these are higher than for *f*CNT/CE, underlying the importance of PMG in the film. The Warburg resistance, Z_w, is lowered with PMG present, from 2.4 for *f*CNT/CE to 0.7 and 1.3 Ω cm^2 s$^{\alpha-1}$ for *f*CNT/PMG/CE and PMG/*f*CNT/CE, respectively.

EIS indicates that electrode platforms combining both PMG and *f*CNT have similar impedance characteristics with significantly lower diffusional resistance and higher pseudocapacitance values than one-component modified electrodes. A close comparison between *f*CNT/PMG/CE and PMG/*f*CNT/CE, reveals slightly lower R_{ct} and Z_w values with *f*CNT on top of PMG, and the highest film capacitance CPE_f for PMG on top of *f*CNT. These results suggest that either electrode architecture can be used for sensor application, the final choice depending on factors such as available surface area, as will be seen below.

3.3. Application of *f*CNT/PMG/CE and PMG/*f*CNT/CE for determination of acetaminophen and pyridoxine

3.3.1. Acetaminophen

Electrochemical methods have been widely used for acetaminophen (ACOP) determination, with many attempts to improve sensor selectivity and sensitivity by using carbon nanotubes [32–41]. Redox polymers have been successfully employed to improve analytical selectivity [2]. Here, the electrodes modified by PMG and *f*CNT were used for paracetamol determination by DPV and fixed potential amperometry.

Typical DPV scans at PMG/*f*CNT/CE are shown in Fig. 4a, with the corresponding calibration plot as inset. The sensitivity of the sensor was 3640 ± 175 μA cm^{-2} mM^{-1} (RSD = 4.8%, n = 3) and the

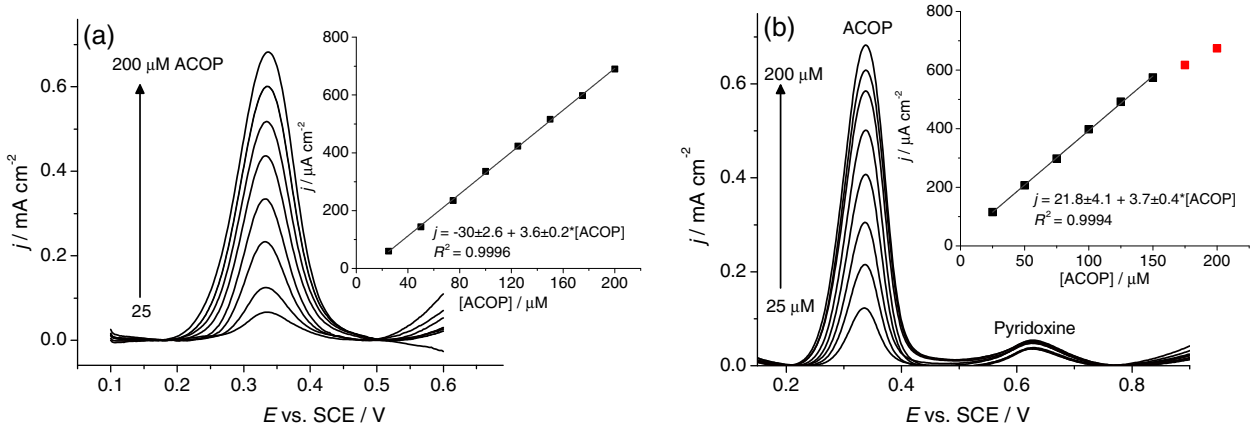

Fig. 4. DPVs recorded at PMG/*f*CNT/CE for increasing concentrations of ACOP (a) in the absence and (b) in the presence of 0.2 mM pyridoxine; corresponding calibration plots in inset.

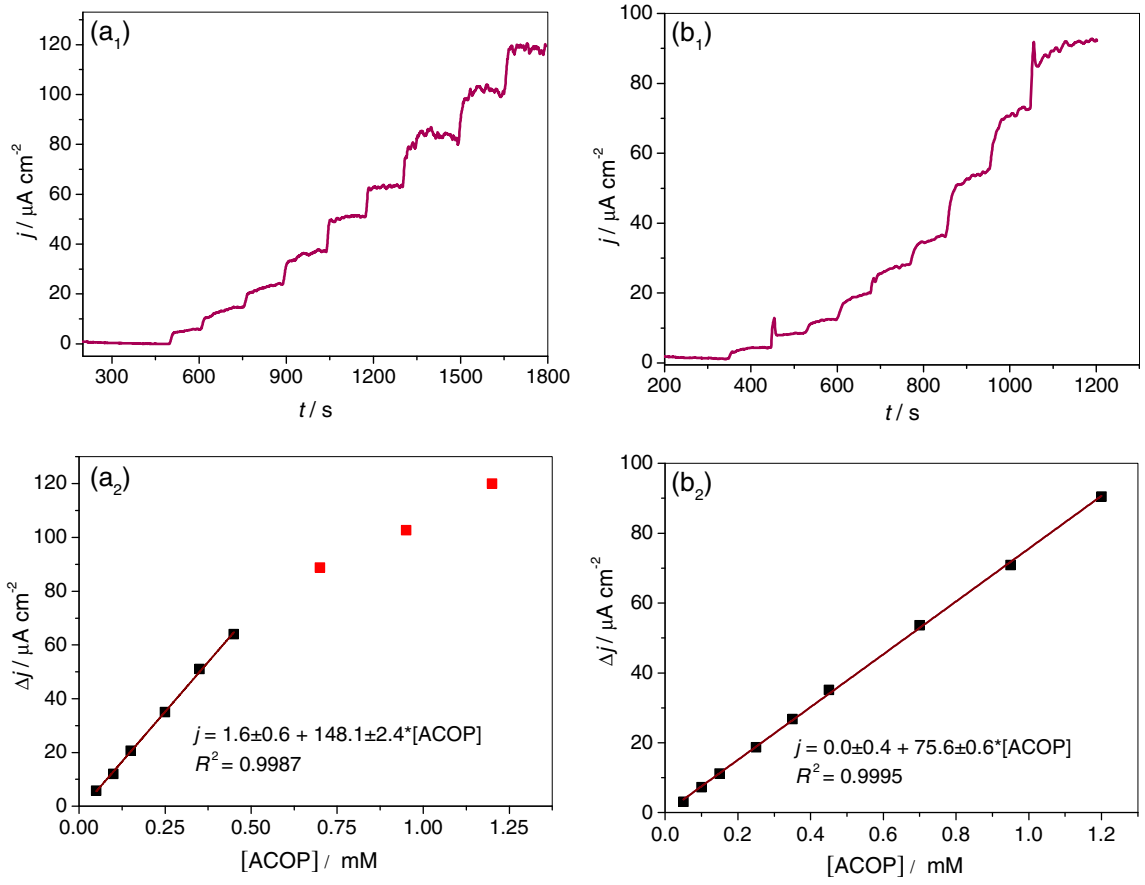

Fig. 5. Fixed potential amperometry at (a_1) *f*CNT/PMG/CE and (b_1) PMG/*f*CNT/CE for increasing concentrations of ACOP; (a_2) and (b_2) corresponding calibration plots. Applied potential + 0.30 V vs. SCE.

detection limit 4.3 ± 0.6 μM (RSD = 13.9%, n = 3), calculated as 3.3 times the standard error divided by the slope of the calibration plot [42]. A lower sensitivity of 920 μA cm^{-2} mM^{-1} was achieved on *f*CNT deposited on top of the polymer, *f*CNT/PMG/CE, which had a detection limit of 9.3 ± 1.1 μM (RSD = 11.8%, n = 3). At the bare CE, the sensitivity was 176 μA cm^{-2} mM^{-1}, while at CE modified only with one component it was 750 at *f*CNT/CE and 380 μA cm^{-2} mM^{-1} at PMG/CE, lower than at either electrode modified with both components, which underlines the importance of combining PMG with *f*CNT to improve sensor performance. The upper limit of the linear range was up to at least 200 μM for all tested sensors. The same analytical properties were achieved at PMG/*f*CNT/CE when ACOP was determined in the presence of 0.2 mM pyridoxine (see DPVs in Fig. 4b), with sensitivity 3.7 mA cm^{-2} μM^{-1}and LoD of 3.9 μM, with the difference that saturation occurred at 150 μM ACOP.

Fixed potential amperometry was also used to investigate both sensor performances, at +0.3 V vs. SCE, very close to the oxidation potential of ACOP in DPV experiments; typical chronoamperograms are displayed in Fig. 5 with corresponding calibration plots.

Table 2
Comparison of PMG/*f*CNT/CE performance with other CNT based acetaminophen (ACOP) sensors, published since 2012.

Electrode architecture		Technique, pH	Sensitivity/μA cm^{-2} mM^{-1}	LoD/μM	References
MWCNT/5ADB/PE		DPV, pH 7.0	341.8	0.2	[32]
CNT-PCPE		SWV, pH 5.0	–	1.1	[33]
MWCNT/Mo^{VI}/PE		DPV, pH 7.0	494.5	0.08	[34]
Graphene nanosheet/SWCNT/GCE		DPV, pH 7.0	–	0.04	[35]
MWCNT(surfactant)/PE		DPV, pH 7.7	–	0.6	[36]
SWCNT$_{magnetic\ entrapment}$/AuSPE	MP 1	CV, pH 7.5	15,000	0.2	[37]
	MP 2			0.2	
	MP 3			0.1	
EF-NiO/MWCNT/PE		SWV, pH 6.0	2333	0.5	[38]
MWCNT/IM/GCE		DPV, pH 7.0	–	–	[39]
MWCNT_graphite/PE		SWV, pH 6.0	–	0.8	[40]
MWCNT_ED_LBL/GCE		DPV, pH 7.0	2.3	0.09	[41]
PMG/*f*MWCNT/GCE		DPV, pH 7.0	3640	4.3	Present work

CNT/5ADB/PE – 5-amino-3,4-dimethylbiphenyl-2-ol CNT paste electrode; CNT-PCPE – CNT poly(aminophenol) paste electrode; AuSPE – Au screen printed electrode; MP – magnetic nanoparticles: 1 – type MayOne T1, 2 – type MayOne C1 and 3 – type M270; EF-NiO/MWCNT/PE – Ethynylferrocene–NiO/MWCNT nanocomposite modified carbon paste electrode; IM-4-(1H-benzo[d]imidazol-2-ylthio)-5-methylbenze-1,2-diol; MWCNT_ED_LBL layer by layer of ethylenediamine and MWCNT.

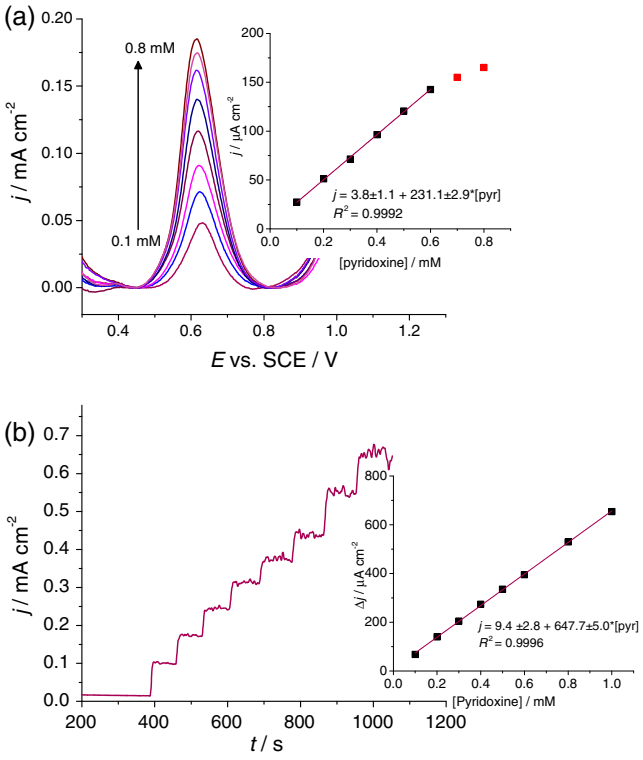

Fig. 6. (a) DPV and (b) fixed potential amperometry at +0.6 V vs. SCE at PMG/*f*CNT/CE for increasing concentrations of pyridoxine; corresponding calibration plots in inset.

As observed, *f*CNT/PMG/CE had a higher sensitivity than PMG/*f*CNT/CE: 139 compared with 75.6 μA cm^{-2} mM^{-1}. Nevertheless, with *f*CNT on top, saturation of sensor response occurs for concentrations higher than 0.75 mM, due to adsorption within the *f*CNT layer, while in the opposite configuration with PMG on top of *f*CNT, no saturation was observed up to 1.2 mM.

As expected, the DPV technique was more sensitive, but whereas in DPV with polymer on top, the sensitivity was higher, in fixed-potential amperometry, the opposite was true. This may be explained if ACOP oxidation occurs on the surface of PMG and by the timescales of the techniques. In amperometric experiments, there is sufficient time for the analyte to diffuse through the upper *f*CNT chitosan layer, some accumulation of ACOP in the CNT layer being possible, which makes this sensor more sensitive than the one with PMG on top. On the other hand, in DPV the timescale of the experiment is much shorter, so that the sensor with PMG on top is more sensitive, the one with *f*CNT on top having the disadvantage of there being insufficient time for ACOP to diffuse to the PMG underneath.

The analytical parameters of the PMG/*f*CNT/CE sensor were compared with other *f*CNT based ACOP sensors, published in the last 3 years [32–41], Table 2. Even though the detection limits were lower for the other sensors, only one exhibited a higher sensitivity, demonstrating the good performance of the developed sensor.

3.3.2. Pyridoxine

The sensor with best analytical properties for ACOP determination was chosen for pyridoxine detection. Typical DPV scans for increasing concentrations of pyridoxine are shown in Fig. 6a, with the corresponding calibration plot in inset. The sensor had a linear response up to 0.6 mM pyridoxine, with a sensitivity of 231 ± 10 (RSD = 4.1%, n = 3) μA cm^{-2} mM^{-1} and a detection limit of 9.4 ± 1.4 (RSD = 14.8%, n = 3) μM. By fixed potential amperometry, at +0.6 V vs. SCE (see Fig. 6 b-inset calibration plot), the sensitivity was ~3 times higher, 648 ± 40 (RSD = 6.1%, n = 3) μA cm^{-2} mM^{-1}, with no saturation up to 1.0 mM, but with a higher LD of 20.4 ± 2.8 (RSD = 13.7%, n = 3) μM. At bare CE, the sensitivities were much lower (91.3 and 3.2 μA cm^{-2} mM^{-1}, by DPV and fixed potential amperometry respectively).

There are not many sensors for vitamin B6 reported in the literature, some being reported in 2003–2005, with a gap until 2010. The analytical performance of the new sensor is compared to those reported after 2010 [43–48] in Table 3. The sensitivity is far superior to the other sensors, except for a C_ceramic/PBNP electrode [43], which operated at a very positive potential of +1.0 V, with a sensitivity of 970 μA cm^{-2} mM^{-1} and a CE/Graphite_PU [44], which had a sensitivity of 1071 μA cm^{-2} mM^{-1} in acetate buffer pH 4.0.

3.3.3. Application of PMG/fCNT/CE sensor to acetaminophen and pyridoxine in pharmaceutical samples

Analytical assays were performed to verify the applicability of the developed sensor to pharmaceutical samples, by standard addition, in order to minimize influence of the matrix. An aliquot of the samples was injected into the buffer electrolyte followed by chosen amounts of acetaminophen or pyridoxine. The time interval between injections was 60–80 s. The declared concentration values of the compounds were 500 mg acetaminophen and 50 mg pyridoxine per tablet, and the values found were 502 ± 2 and 47.6 ± 0.9 mg per tablet for acetaminophen and pyridoxine, respectively, in good agreement with the declared acetaminophen and pyridoxine content of the tablets. In order to establish the

Table 3
Comparison of PMG/*f*CNT/CE performance with other pyridoxine sensors, published since 2010.

Electrode architecture	Technique, pH	Sensitivity/μA cm^{-2} mM^{-1}	LoD/μM	References
PBNP/C_ceramic	Amp. +1.0 V, Ac, pH 4.0	970	0.5	[43]
MWCNT/AuNP/GCE	DPV, PBS pH 7.0	–	3.1	[26]
Graphite_PU	SWV, Ac, pH 4.2	1071.4	0.7	[44]
ssDNA/GCE	CV, NaOH	469.5	40	[45]
PEDOT(doped)/GCE	DPV, PBS pH 7.0	42.3	–	[46]
ZrO_2NP/PEDOT/GCE	DPV, PBS pH 7.0	60.6	0.2	[47]
SPE-C	DPV, Ac, pH 5.0	103.5	3.3	[48]
MWCNT/SPE-C		135.4	1.5	
SWCNT/SPE-C		199.0	6.8	
PMG/*f*CNT/GCE	Amp. +0.6 V, PBS pH 7.0	648	18.5	Present work
	DPV, PBS pH 7.0	232	9.4	

PBNP/C_ceramic – Prussian Blue nanoparticles modified carbon ceramic electrode; Ac – acetate buffer, AuNP_Au nanoparticles; Graphite PU – graphite polyurethane electrodes; PEDOT(doped) – Poly(3,4-ethylenedioxythiophene) doped with ClO_4^-, Fc^- or $Fe(CN)_6$; ZrO_2NP – ZrO_2 nanoparticles; SPE – screen printed electrodes.

Table 4
Determination of acetaminophen and pyridoxine in pharmaceutical formulation.

Sample	Added/μM	Found/μM	Recovery/%
Acetaminophen	0	200 ± 1	–
	50	251 ± 1	102.0
	100	298 ± 1	98.2
	150	352 ± 1	101.5
Pyridoxine	0	120 ± 1	–
	50	172 ± 1	104.2
	100	223 ± 1	103.3
	150	275 ± 1	103.5

suitability of the proposed method, the recovery rates were also calculated and are presented in Table 4. The recovery rates close to 100% indicate that the modified electrode can be efficiently used for the determination of both compounds in pharmaceutical preparations.

4. Conclusions

New electrode architectures were developed on composite electrode substrates modified with electropolymerised poly(methylene green) and with *f*CNT entrapped in a chitosan layer, in two configurations *f*CNT/PMG/CE and PMG/*f*CNT/CE. PMG polymerizes better on *f*CNT/CE than on CE, the higher peak currents indicating more polymer growth at PMG/*f*CNT/CE. Analysis of impedance spectra shows that electrode platforms containing both PMG and *f*CNT are superior to those with only one component, for application as sensors. For the determination of ACOP, DPV led to higher sensitivities than fixed potential amperometry, that with best analytical performance being at PMG/*f*CNT/CE, which was also chosen for determination of pyridoxine, where fixed-potential amperometry was better than DPV. For pyridoxine, analytical parameters significantly superior to those in the literature were achieved. Both analytes were successfully determined in pharmaceutical samples by the standard addition method, underlying the reliability of the present analytical method.

Conflict of interest

The authors of the present article have no conflict of interests to declare.

Acknowledgements

Financial support from Fundação para a Ciência e a Tecnologia (FCT), Portugal PTDC/QUI-QUI/116091/2009, POCH, POFC-QREN (co-financed by FSE and European Community FEDER funds through the program COMPETE – Programa Operacional Factores de Competitividade under the projects PEst-C/EME/UI0285/2013) and CENTRO-07-0224 -FEDER-002001 (MT4MOBI)) is gratefully acknowledged. M.M.B. thanks FCT for postdoctoral fellowships SFRH/BPD/72656/2010 and C.T.T. thanks the Brazilian National Council for Scientific and Technological Development, CNPq-Brazil, for a grant under the programme "Ciência sem Fronteiras".

References

[1] B.P. Nikolskii, V.V. Palchevskii, L.A. Polyanskaya, A.G. Rodichev, Dokl. Akad. Nauk SSSR 194 (1970) 1334–1337.
[2] R. Pauliukaite, M.E. Ghica, M.M. Barsan, C.M.A. Brett, Anal. Lett. 43 (2010) 1588–1608.
[3] M.N. Arechederra, C. Jenkins, R.A. Rincón, K. Artyushkova, P. Atanassov, S.D. Minteer, Electrochim. Acta 55 (2010) 6659–6664.
[4] H. Li, H. Wen, S.C. Barton, Electroanalysis 24 (2012) 398–406.
[5] V. Svoboda, M. Cooney, B.Y. Liaw, S. Minteer, E. Piles, D. Lehnert, S.C. Barton, R. Rincon, P. Atanassov, Electroanalysis 20 (2008) 1099–1109.
[6] C.W. Narváez Villarrubia, R.A. Rincón, V.K. Radhakrishnan, V. Davis, P. Atanassov, ACS Appl. Mater. Interfaces 3 (2011) 2402–2409.
[7] R.A. Rincón, C. Lau, K.E. Garcia, P. Atanassov, Electrochim. Acta 56 (2011) 2503–2509.
[8] P. Kar, H. Wen, H.Z. Li, S.D. Minteer, S.C. Barton, J. Electrochem. Soc. 158 (2011) B580–B586.
[9] P.G. Fenga, F.P. Cardoso, S. Aquino Neto, A.R. De Andrade, Electrochim. Acta 106 (2013) 109–113.
[10] J. Yu, M. Rasmussen, S.D. Minteer, Electroanalysis 25 (2013) 1130–1134.
[11] A.E. Blackwell, M.J. Moehlenbrock, J.R. Worsham, S.D. Minteer, J. Nanosci. Nanotechnol. 9 (2009) 1714–1721.
[12] H. Atamna, A. Nguyen, C. Schultz, K. Boyle, J. Newberry, H. Kato, B.N. Ames, FASEB J. 22 (2008) 703–712.
[13] C.B. Jacobs, M.J. Peairs, B.J. Venton, Anal. Chim. Acta 662 (2010) 105–127.
[14] Z. Wang, M. Etienne, S. Pöller, W. Schuhmann, G.-W. Kohring, V. Mamane, A. Walcarius, Electroanalysis 24 (2012) 376–385.
[15] R. Pauliukaite, M.E. Ghica, O. Fatibello-Filho, C.M.A. Brett, Anal. Chem. 81 (2009) 5364–5372.
[16] M.E. Ghica, R. Pauliukaite, O. Fatibello-Filho, C.M.A. Brett, Sens. Actuator B – Chem. 142 (2009) 308–315.
[17] R. Pauliukaite, M.E. Ghica, O. Fatibello-Filho, C.M.A. Brett, Comb. Chem. High Throughput Screen 13 (2010) 590–598.
[18] K.A. Worsley, I. Kalinina, E. Bekyarova, R.C. Haddon, J. Am. Chem. Soc. 131 (2009) 18153–18158.
[19] H. Yi, L.-Q. Wu, W.E. Bentley, R. Ghodssi, G.W. Rubloff, J.N. Culver, G.F. Payne, Biomacromolecules 6 (2005) 2881–2894.
[20] A. Wade (Ed.), Martindale, The Extra Pharmacopoeia, 27th ed., The Pharmaceutical Press, London, 1979.
[21] Q. Wan, X. Wang, F. Yu, X. Wang, N. Yang, J. Appl. Electrochem. 39 (2009) 1145–1151.
[22] M.V.H. Hashmi, Assay of Vitamins in Pharmaceutical Preparations, Wiley, London, 1973. pp. 188–212.
[23] J. Gonzalez-Rodriguez, J.M. Sevilla, T. Pineda, M. Blazquez, Int. J. Electrochem. Sci. 7 (2012) 2221–2229.
[24] M.F.S. Teixeira, A. Segnini, F.C. Moraes, L.H. Marcolino-Júnior, O. Fatibello-Filho, E.T.G. Cavalheiro, J. Braz. Chem. Soc. 14 (2003) 316–321.
[25] W. Qu, K. Wu, S. Hu, J. Pharm. Biomed. Anal. 36 (2004) 631–635.
[26] Y. Zhang, Y. Wang, Am. J. Anal. Chem. 2 (2011) 194–199.
[27] R.L.R.P. Fagury, K.O. Lupetti, O. Fatibello-Filho, Anal. Lett. 38 (2005) 1857–1867.

[28] C. Gouveia-Caridade, R. Pauliukaite, C.M.A. Brett, Electrochim. Acta 53 (2008) 6732–6739.
[29] M.M. Barsan, E.M. Pinto, C.M.A. Brett, Electrochim. Acta 53 (2008) 3973–3982.
[30] Q. Li, J. Zhang, H. Yan, M. He, Z. Liu, Carbon 42 (2004) 287–291.
[31] E. Barsoukov, Impedance Spectroscopy. Theory Experiment and Applications, second ed., in: J.R. Macdonald (Ed.), Wiley, New York, 2005.
[32] H. Beitollahi, A. Mohadesi, S. Mohammadi, A. Akbari, Electrochim. Acta 68 (2012) 220–226.
[33] I. Noviandri, R. Rakhmana, Int. J. Electrochem. Sci. 7 (2012) 4479–4487.
[34] H. Beitollahi, I. Sheikhshoaie, Mater. Sci. Eng. C-Mater. Biol. 32 (2012) 375–380.
[35] X. Chen, J. Zhu, Q. Xi, W. Yang, Sens. Actuat. B – Chem. 161 (2012) 648–654.
[36] F.F. Hudari, E.H. Duarte, A.C. Pereira, L.H. Dall'Antonia, L.T. Kubota, C.R.T. Tarley, J. Electroanal. Chem. 696 (2013) 52–58.
[37] R. Olivé-Monllau, F.X. Muñoz-Pascual, E. Baldrich, Sens. Actuat. B – Chem. 185 (2013) 685–693.
[38] M.R. Shahmiria, A. Baharia, H. Karimi-Malehb, R. Hosseinzadeh, N. Mirnia, Sens. Actuat. B – Chem. 177 (2013) 70–77.
[39] N. Nasirizadeh, Z. Shekari, H.R. Zare, M.R. Shishehbore, A.R. Fakhari, H. Ahmar, Biosens. Bioelectron. 41 (2013) 608–614.
[40] M. Keyvanfard, R. Shakeri, H. Karimi-Maleh, K. Alizad, Mater. Sci. Eng. C – Biomim. 33 (2013) 811–816.
[41] Y. Li, S. Feng, S. Li, Y. Zhang, Y. Zhong, Sens. Actuator B – Chem. 190 (2014) 999–1005.
[42] J.C. Miller, J.N. Miller, Statistics and Chemometrics for Analytical Chemistry, 5th ed., Pearson Prentice Hall, Edinburgh, 2005.
[43] H. Razmi, R. Mohammad-Rezaei, Electrochim. Acta 55 (2010) 1814–1819.
[44] C.A. Fonseca, G.C.S. Vaz, J.P.A. Azevedo, F.S. Semaan, Microchem. J. 99 (2011) 186–192.
[45] S.-Q. Liu, W.-H. Sun, L.-C. Li, H. Li, X.-L. Wang, Int. J. Electrochem. Sci. 7 (2012) 324–337.
[46] T. Nie, J.-K. Xu, L.-M. Lu, K.-X. Zhang, L. Bai, Y.-P. Wen, Biosens. Bioelectron. 50 (2013) 244–250.
[47] T. Nie, K. Zhang, J. Xu, L. Lu, L. Bai, J. Electroanal. Chem. 717–718 (2014) 1–9.
[48] B. Brunetti, E. Desimoni, J. Food Compos. Anal. 33 (2014) 155–160.